

Age and metallicity gradients in the Galactic Bulge [★]

A differential study using HST/WFPC2

Sofia Feltzing^{1,2,3} and Gerard Gilmore²

¹ Royal Greenwich Observatory Madingley Road, Cambridge CB3 0EZ, U.K.

² Institute of Astronomy, Madingley Road, Cambridge CB3 0HA

³ Present address: Lund Observatory, Box 43, S-221 00 Lund, Sweden

Received 06-03-1998; accepted 22-12-1999

Abstract. The Galactic Bulge has long been assumed to be a largely old stellar population. However, some recent studies based on observations with the HST WF/PC-1 and WFPC2 of stars in the Galactic Bulge have concluded that the old population may not make up more than 30% of the total. Other studies using HST/WFPC2 differential studies of ‘Bulge’ globular clusters and field stars have found the bulge to be comparable in age to the Galactic Halo. A complication in all these studies is the presence of a substantial population of stars which mimic a young bulge population, but which may be, and are often assumed to be, foreground disk stars whose reddening and distance distributions happen to mimic a young bulge turnoff. We show, using number counts in HST/WFPC2 colour-magnitude diagrams of both field stars in the Bulge and of two ‘bulge’ and one ‘disk’ globular cluster (NGC6528, NGC6553, and NGC5927) that the stars interpreted as young in fact are foreground disk stars. Thus, we confirm that the bulk of the bulge field stars in Baade’s Window are old. The existence of a young *metal-rich* population cannot, however, be ruled out from our data.

We also test for age and metallicity gradients in the Galactic Bulge between the two low extinction windows Baade’s window ($\ell=1^\circ.1, b=-4^\circ.8$) and Sagittarius-I ($\ell=1^\circ.3, b=-2^\circ.7$). We use the colour-magnitude diagram of a metal-rich globular cluster as an empirical isochrone to derive a metallicity difference of $\lesssim 0.2$ dex between Baade’s window and SGR-I window. This corresponds to a metallicity gradient of $\lesssim 1.3$ dex/kpc, in agreement with recent near-IR CMD studies. Such a steep gradient, if de-

tected, would require the existence of a short scale length inner component to the Bulge, most likely that prominent in the near infra red, which perhaps forms a separate entity superimposed on the larger, optical Bulge as observed in Baade’s window.

Key words: Galaxy: abundances, center, general, globular clusters: NGC5927, NGC6528, NGC6553, stellar content

1. Introduction

The nature and origin(s) of Galactic Bulges are key aspects of any galaxy formation model, and of the Hubble galaxy classification sequence. However, the present-day properties of bulges in spiral galaxies are not well known (eg Silk & Wyse 1993; Wyse, et al. 1997). Do bulges form late, early or continuously? Are bulges related to halos? To disks? Are they single stellar populations? The existence of smooth and/or discontinuous gradients in age and/or metallicity in the stellar population(s) in the Galactic Bulge can help to discriminate between these different scenarios, and is the topic of this paper.

Is there evidence for the widely repeated assumption that the Galactic Bulge is old? Recently published colour magnitude diagrams from HST/WFPC2 and HST/WFC1 of the Galactic Bulge and the bulge globular clusters (Valenari et al. 1996, Ortolani et al. 1995, Holtzman et al 1993) while dominated by fairly old stars, show a substantial population of stars above the dominant old turnoff. Are these foreground disk stars, or is there a minority very young bulge population? Since even a minority young bulge population is of interest, we examine here the limits on young stars in the bulge windows.

One common approach to determine the properties of the Bulge is to study the so called bulge globular clusters

Send offprint requests to: Sofia Feltzing

[★] Based on observations with the NASA/ESA Hubble Space Telescope, obtained at the Space Telescope Science Institute, which is operated by the Association of Universities for Research in Astronomy, Inc. under NASA contract No. NAS5-26555

(see e.g. Zinn 1996, Ortolani et al. 1995, Minniti 1996). While primarily motivated by observational convenience, the rationale behind this approach is the assumption that these clusters may be valid tracers of the stellar population(s) of the Bulge (see however Zinn 1996 and Harris 1998) Formation scenarios relevant to this approach include the possibility that the Bulge has been assembled from numerous such clusters and these are the last surviving (Gnedin & Ostriker 1997), or that the clusters formed a system associated with the Bulge rather than with the rest of the spheroidal component(s) of the Galaxy. Thus the idea is that we may be able to infer the age and/or metallicity of the Bulge stellar population either directly from studies of these clusters, or through differential studies of the clusters and field stars, under the assumption of similar metallicity. Since there is no *ab initio* understanding of the formation of either galactic bulges or globular clusters, and the age range of the globular cluster system remains a topic of active debate, such analyses merit close scrutiny. The most recent and extensive such analysis is that of Ortolani et al. (1995, 1996) who observed two such globular clusters, NGC6553 and NGC6528, with HST/WFPC2, and deduced that the Bulge has the same age as the Halo.

Analysis of suitably-chosen globular clusters introduces several possible complications. The first is the major problem of defining a proper population of ‘bulge’ globular clusters. Some of the clusters used, e.g. Ter7, have recently been shown to be associated with the satellite dwarf galaxy Sgr dSph, rather than with the Galaxy itself. They may therefore not be representative of the Galactic Bulge. The method of comparing ridge-lines of globular clusters to infer relative ages requires the clusters in question to have similar metallicities, and relative chemical abundances of the alpha-elements, to avoid an age-metallicity degeneracy (Stetson et al. 1996, Vandenberg et al. 1990, 1996). New results by Cohen et al. (1999) show that NGC6553 may be as much as ~ 0.5 dex more metal-rich than 47 Tuc, illustrating the potentially large effects of metallicity range. The impressive recent study of Rosenberg et al. (1999), indicating a dispersion in ages for the intermediate metallicity globular clusters, and a large systematic age difference between the metal-rich and metal-poor clusters illustrates the complexity.

Another potential uncertainty is that the metallicity distribution function of the stars in the galactic Bulge is more similar to that in the solar-neighbourhood (cf. Wyse and Gilmore 1995) than to that for clusters within 5 degrees of the Galactic centre (Minniti 1996; Barbuy et al. 1998). The bulge cluster distribution is both more narrow and less metal-rich than the bulge field stars, complicating any direct comparison.

Clearly, if one wishes to know the age of the bulge field stars, it is desirable to observe the stars in the Bulge directly. Direct studies of the Bulge are difficult due to the severe crowding towards the central regions of the Galaxy

and the large, patchy, reddening along the line of sight. Several detailed studies of the outer Galactic Bulge exist, providing kinematics and chemical abundance distribution functions (Ibata and Gilmore 1995a, 1995b; Minniti et al. 1995; see also Wyse et al. 1997). For the inner Bulge several analyses of the low reddening Baade’s window are available (e.g. Ortolani et al. 1995, Vallenari et al. 1996, Holtzman et al. 1993, Terndrup 1988, Ng et al. 1996), with direct studies of the inner bulge field stars in the near-IR recently also becoming available (Frogel et al. 1999), and even mid-IR ISO photometry (Omont et al. 1999, Glass et al. 1999). Additionally, many recent studies have emphasized the high continuing rate of star formation in the inner bulge/disk. Do these stars diffuse with time the few hundred parsecs into the Sgr and Baade’s windows?

The interpretation of extant data is unclear, with a variety of contradictory results. Vallenari et al. (1996) use a mixture of WF/PC-1 and NTT data while Holtzman et al. (1993) rely exclusively on (the same) WF/PC-1 data. Both groups reached the conclusion that the Bulge is dominated by a significant young stellar populations. Ortolani et al. (1995) using similar NTT data for Baade’s Window found the Bulge to be as old as the Halo.

The confusion among the results from the space based observations should be contrasted with ground based optical observations which find little evidence for a substantial young stellar population(s) in the Galactic Bulge (eg Terndrup 1988), albeit rather far from the centre. Note however that these observations do not cover the main-sequence turn-off and the results are based on the giant branch. The main-sequence turn-off is more sensitive to detection of a significantly younger stellar populations. Further complication is provided by studies of OH/IR stars, suspected to be of intermediate age, which are common in the inner bulge, or disk (Sevenster et al. 1997).

The distribution function of chemical abundances is a key parameter defining a stellar population. In the outer Galactic Bulge Ibata & Gilmore (1995b) derived the relevant distribution function from spectroscopy of K giants. They found a mean abundance of ~ -0.2 dex, with a very wide dispersion. In Baade’s window McWilliam & Rich (1994) and Sadler et al. (1996) provided similar results. Sadler et al. (1996) found for 400 K giants a mean abundance of $[\text{Fe}/\text{H}] = -0.11 \pm 0.04$ dex, with more than half the sample in the range $-0.4 < [\text{Fe}/\text{H}] < +0.3$ dex. This is similar to the results from the detailed spectroscopic analysis of McWilliam & Rich (1994). A metallicity gradient has been suspected for fields outside Baade’s Window, Terndrup (1988) and Minniti et al. (1995). The important conclusion from the spectroscopic analyses is that the stellar populations of the inner Galactic Bulge are complex, and that their analysis requires careful consideration of projected disk and other populations.

In this paper we study colour-magnitude diagrams, derived from archival HST/WFPC2 images, for 4 fields and two clusters towards the Galactic Bulge and one ‘disk’

cluster. We perform a purely differential study of the properties of the Galactic Bulge population(s), quantifying any systematic offsets and/or gradients in age and/or metallicity in the field population(s).

The paper is organized as follows; in Sect. 2 we detail the observations used and in Sect. 3 describe how we derive the photometric magnitudes from the images. Sect. 4 discusses reddening and distances for the individual fields and clusters, and the utility of the cluster data. Sect. 5 discusses the age of the Bulge, while Sect. 6 asks the question whether a metallicity gradient might be present in the inner Bulge. Sect. 7 includes a summarizing discussion which puts our results into the context of other studies. A brief summary is found in Sect. 8.

2. The data

All observations analyzed here were obtained from the HST-archive. The observations for the two clusters, NGC6528 and NGC6553, have previously been reported and discussed in Ortolani et al. (1995) and the observation of NGC5927 in Fullton et al. (1996). However, to get a set of data which is consistently treated we have derived our own photometry from the original images. The images are detailed in Table 1, and their positions on the sky are shown in Fig. 1. The results presented here are all, due to the crowding in some of the fields, based exclusively on the PC1 images.

2.1. Data reductions

All frames have been recalibrated through the STScI pipeline calibration for HST at the Space Telescope - European Coordinating Facility, using the most suitable flat field and bias frames available.

2.2. Combining images

Because the WFPC2 images are under-sampled extra care has to be exercised so that counts in the centre of stars are not lost when images are combined in order to remove cosmic rays. Sub-pixel shifts between two images can cause the centre flux in one image (or in both) to look like a cosmic ray when the images are compared in the cosmic ray algorithm. Experiments on several of the image sets, using the `stdas.hst.calib.wfpc.crrej` task, showed that up to 10% of the counts may be lost unless a term linear in the counts (scalenoise) is included in the modeling of σ used in the rejection algorithm (see the help file for `CRREJ`).

3. Stellar Photometry: Deriving colour-magnitude diagrams

To derive photometric magnitudes we have used the standard IRAF¹ tasks in the DAOPHOT package. To calibrate

¹ IRAF is distributed by National Optical Astronomy Observatories, operated by the Association of Universities for Re-

our data we have used the procedures detailed in Holtzman et al. (1995b), as well as empirical determinations of aperture corrections.

We follow the general procedure of first detecting possible stars with DAOFIND, derive initial photometric magnitudes from aperture photometry using PHOT, derive an analytical point-spread-function (*psf*) for each image (assumed constant over the entire chip) and finally perform *psf*-fitting on the list of possible stars to determine stellar magnitudes using ALLSTAR. The initial aperture photometry is done in an aperture of 2 pixels. We use the *psf*-fitted magnitudes in our analysis. The raw *psf*-fitted magnitudes need to be corrected for a number of effects which are peculiar to HST, and calibrated onto the HST in-flight system.

For the observations at $(l, b) = (2^{\circ}9, -7^{\circ}95)$ only one observation in the F606W passband was available. We identified the objects on the combined F814W image and used that list to identify the stars on which to perform measurements in the F606W image. The colour-magnitude diagram was then searched for anomalous looking stars, which were inspected by eye in both passbands and if deemed to be contaminated by cosmic rays, excluded.

We first present the steps in our calibration and then discuss and detail each step separately as some of the steps are non-trivial. Our calibration contains the following steps;

1. apply empirical correction for the difference between aperture and *psf*-fitted magnitudes,
2. add 2 electrons to the flux in each pixel inside a radius of 5 pixels,
3. correct for the CTE effect,
4. correct for the geometric distortion,
5. normalize to WF3 and bay 4 (if applicable),
6. apply Holtzman's synthetic aperture corrections from 5 pixels out to 11 pixels ($0''.5$),
7. add synthetic zero points from Holtzman et al.

3.1. Aperture vs *psf*-photometry (*ap/psf*)

There is usually a zero-point offset (as well as a spread) between magnitudes derived from *psf*-fitting and from aperture measurements. Since we construct our own *psf* from the frame itself this offset is due to the magnitude assigned to the *psf* by the PSF task. This magnitude is the magnitude of the first star used in constructing the *psf*, thus it is somewhat arbitrary. This also means that the offset between aperture photometry and *psf*-fitted photometry may not always be the same or even have the same sign in two frames.

For the stars that had been used to create the analytic *psf* we measured aperture magnitudes inside 5 pixels and

search in Astronomy, Inc., under contract with the National Science Foundation, USA.

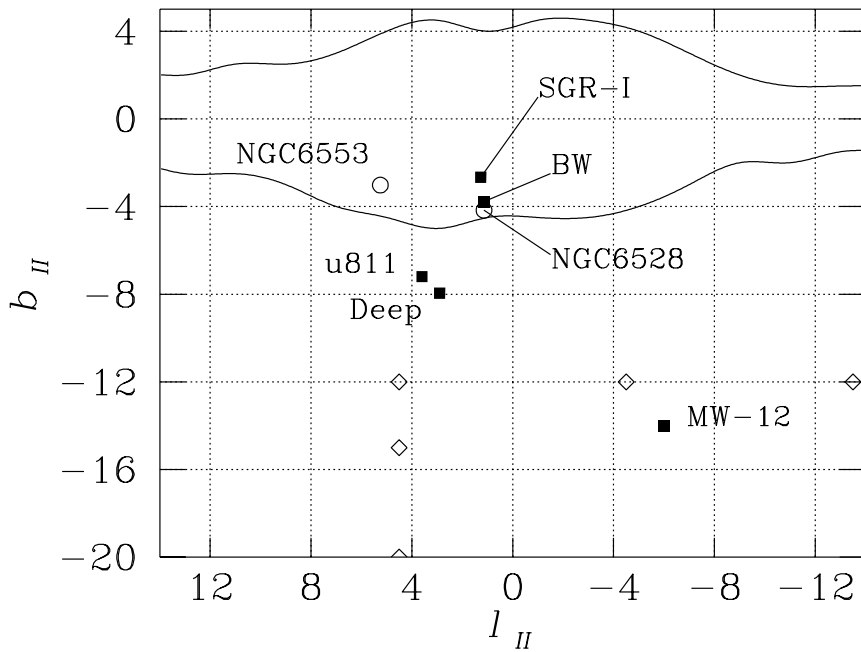


Fig. 1. Positions of fields and clusters. Clusters are denoted by open circles and fields by filled squares. NGC5927 (with $l = -34^\circ$) is well outside this map. We also show the positions of the 5 inner-most fields studied by Ibata and Gilmore (1995a,b), denoted by open diamonds. The Sgr dSph has its major axis along $l = +5^\circ$, and extends down to $b \lesssim 4^\circ$

Table 1. Coordinates and passbands of observations for the fields and clusters. For the fields we give the coordinates for the centre of the PC1 and for the clusters the coordinates for the cluster centres. the column headed ID give the HST archive identification number of the original observing program in which the observations were obtained. The last column give the total number of stars simultaneously detected in F814 and F555W or F606W according to the selection criteria discussed in Sect.3. If the data were truncated the truncation magnitude is indicated in the last column.

Field	l	b	Passbands	Total exp.time	ID	Date of obs.	F814W+F555W/F606W
SGR-I	$1^\circ 27'$	$-2^\circ 66'$	F814W, F555W	3000,3000	5207	28/08/94	2940
BW	$1^\circ 14'$	$-3^\circ 77'$	F814W, F555W	2000,2000	5105	12/08/94	2221 ($V_{555} < 26$)
			F814W, F555W	80,80	6185	2/09/95	1150 ($V_{555} < 23$)
MW-12	$-6^\circ 00'$	$-14^\circ 00'$	F814W, F555W	1000,1200	6614	9/10/96	63
u811	$3^\circ 60'$	$-7^\circ 20'$	F814W, F606W	2600,2600	5371	14,15/09/97	907
Deep	$2^\circ 90'$	$-7^\circ 95'$	F814W, F606W	5800,2900	6254	1/05/96	463 ($V_{606} < 27$)
NGC5927	$326^\circ 6$ (-34°)	$4^\circ 86'$	F814W, F555W	3200,2400	5366	8/05/94	3289
			F814W, F555W	210,150	5366	8/05/94	3587
NGC6528	$1^\circ 14'$	$-4^\circ 17'$	F814W, F555W	200,100	5436	27/02/94	1824
NGC6553	$5^\circ 25'$	$-3^\circ 02'$	F814W, F555W	200,100	5436	25/02/94	2795

subsequently calculated the difference between these magnitudes and the magnitudes derived from *psf*-fitting, Fig. 2. The scatter around the mean-value for these corrections is ≤ 0.03 magnitudes both in F555W and F814W and for both long and short exposures. The difference was used as an empirical aperture correction. The results are listed in Table 2. The *psf*-magnitudes were in this way corrected out to $0'.5$.

3.2. Long versus short exposures

For the field in Baade’s window a set of images with exposure times of 2×1000 s, 4×200 s and 2×40 s is available. This has made it possible to investigate to what extent the magnitudes derived from long and short exposures

of the same stars (and in this case also in a crowded and reddened field) give the same magnitudes. There is a well-known “feature” of HST photometry that short- and long-exposure magnitudes do not agree in zero-point. An addition of $2e^-/pixel$ to the flux measured in aperture photometry has been suggested as an empirical way of correcting for such a discrepancy. We confirm that this is a practical empirical formula. As we correct out to 5 pixels radius for the discrepancy between aperture and *psf*-fitted magnitudes we add 2 electrons to the flux in each pixel inside that radius.²

² Since this article was first submitted there has been significant development in the understanding of the long-vs-short exposure problem. Further discussion of this problem and

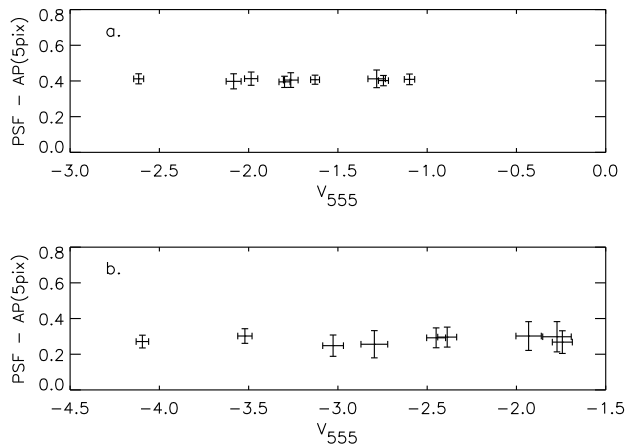


Fig. 2. Difference between *psf*-fitted magnitudes and aperture magnitudes measured inside an aperture with radius 5 pixels as a function of the *psf*-fitted magnitudes. In panel a. we show the data for Baade’s window long exposure and in panel b. short exposure. The error bars show the errors as given by PHOT and ALLSTAR. Note the different ranges on the x-axes.

Table 2. Zero points, aperture corrections from Holtzman et al. (1995a) and corrections for the zero points of the empirical *psfs*.

Quantity	Field	F555W	F606W	F814W
Zero point		21.723	22.084	20.844
Ap.corr.		<u>0.89</u>	<u>0.88</u>	<u>0.87</u>
(Holtzman)		0.96	0.955	0.95
<i>Psf</i> -	SGR-I	0.220	–	0.460
zero-point	BW long	0.296	–	0.406
corr.	BW short	0.281	–	0.470
	MW-12	0.342	–	0.509
	u811	–	0.361	0.485
	Deep	–	0.363	0.434
	NGC5927I	0.303	–	0.493
	NGC5927s	0.240	–	0.469
	NGC6528	0.270	–	0.444
	NGC6553	0.460	–	0.310

3.3. Aperture corrections, Charge Transfer Efficiency (CTE) and Effective pixel area (EPA)

Aperture corrections to $0''.5$ apertures, i.e. 11 pixels on the PC1, from the 5 pixel apertures used to derive the difference between *psf* and aperture magnitudes are employed from Table 2 of Holtzman et al. (1995a).

The CTE has the effect that stellar objects in a given row (more charge transfer) appear fainter than they should

its solution may be found in the WFPC2 Instrument Science Reports 98-02 which can be found at the following URL http://www.stsci.edu/ftp/instrument_news/WFPC2/wfpc2_bib.html

have appeared had they been at a lower row number. This is corrected for through a simple formula suggested by Holtzman et al. (1995a,1995b) which means that at the highest row the detected light is 4% higher than at the first row and this correction changes linearly along the column. For observations taken before the cool down of the CCDs in WFPC2, 32 April 1994, the CTE is higher, $\sim 10\%$.

As discussed in Holtzman et al. (1995a) the WFPC2 cameras have geometric distortions. We correct for these distortions using the information in the map of effective pixel area given in Fig.16, Holtzman et al. (1995a).

3.4. Completeness

In order to determine the level of completeness, as a function of derived apparent magnitude, we have performed the “ADDSTAR experiment”, ie we add artificial stars at a given magnitude, thus creating a new image. The new frames were then put through the same processes as described above and the list of synthetic stars created by ADDSTAR was cross-correlated with the final list of detected stars to reveal how many of the synthetic stars had been recovered. For this we required not only that the coordinates should be the same but also that the new magnitude should be within 0.5 magnitudes of the magnitude assigned to the synthetic star by ADDSTAR, as illustrated in Fig. 3.

Note that in this study we do not require a detailed knowledge of the completeness function. This is because we are studying the turn off regions and brighter in the colour-magnitude diagrams. Our only requirement here is to show that completeness is not a significant problem near the main-sequence turnoff. In fact, our photometry extends several magnitudes fainter than necessary for this experiment.

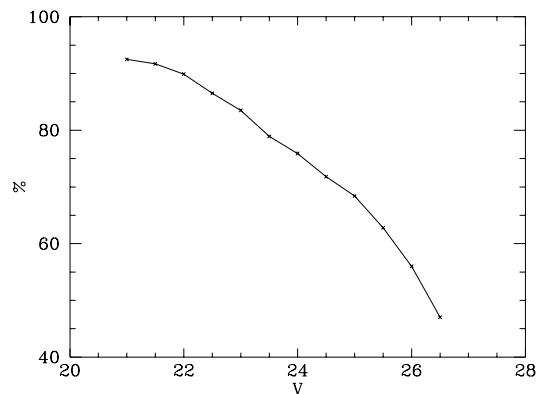


Fig. 3. Completeness for the deep exposure of Baade’s window. SGR-I shows the same level of completeness. This completeness is based on the stars detected in both V_{555} and I_{814}

3.5. Selection of final stellar samples

All images were carefully inspected for saturated stars and spurious detections around saturated stars (mottling) and along the diffraction patterns. It was found that once the data for F814W and F555W were matched very few saturated stars remained in the final sample and virtually no detections on diffraction spikes and in the mottling pattern remained.

The final selection of stellar samples was based on the diagnostic diagrams produced from the *psf*-fitting photometry of which an example is presented in Fig. 4. As can be seen in this figure a cut at $\chi_{814} < 2.5$ and $\chi_{555} < 2.5$ cleans up the error vs. magnitude diagrams satisfactorily.

4. Reddening, distances and metallicities.

As we are using archive data we do not have control over which passbands have been used. This makes it difficult to address the question of reddening for all fields and clusters in a consistent way. We later consider the sensitivity of our conclusions to the adopted reddening. Initially we consider available determinations in the literature.

We have searched the literature for independent determinations of the reddening. For two of the clusters and the SGR-I field observations in the two HST U-passbands exist, which could in principle allow derivation of the extinction directly. Unfortunately the clusters were observed in F336W, which has a large red leak. This means that the extinction has a non-linear dependence on the reddening which makes it difficult to deredden the stars in the colour-colour diagram.

We use the extinction for a K5 spectrum as given in Table 12 of Holtzman et al. (1995b) to calculate the reddening vector. When $E(B - V)$ is not directly available, we use the extinction law given in Table 2 of Cardelli et al. (1989) to derive $E(B - V)$ (adopting $R_V = 3.1$). The extinctions and reddenings from the literature are collected in Table 3.

Table 3. Reddenings from the literature and extinctions, derived from Holtzman et al. (1995b)

Field	$E(B - V)$	A_{F555W}	$E(V_{F555W} - I_{F814W})$
SGR-I	0.58	1.77	0.70
BW	0.49	1.49	0.59
NGC5927	0.46	1.41	0.56
NGC6528	0.6	1.83	0.73
NGC6553	1.0/0.8	3.03/2.45	1.20/0.50

4.1. Comparison with previous studies

The same observations as we use for NGC6553 and NGC6528 have previously been reported in Ortolani et al.

(1995) and those for NGC5927 in Fullton et al. (1996). A comparison between our colour-magnitude diagrams and theirs shows excellent agreement where even individual stars may be identified. The comparison of both the general structure of the colour-magnitude diagrams as well as of magnitudes of individual stars give us confidence in our photometry for the other fields, eg. MW, SGR-I. Ortolani et al. (1995) did not publish the colour-magnitude diagram for NGC6528 but the ridge-line.

4.2. The Bulge fields

4.2.1. SGR-I

SGR-I is a well known low-extinction area. Glass et al. (1995) adopt $A_V = 1.87$. They ascribe fairly large and uncertain errors to this value. The cluster NGC6522 appears to have similar extinction to SGR-I. Walker & Mack (1986) found $A_V = 1.78 \pm 0.10$. Using $R_V = 3.1$ this corresponds to $E(B - V) = 0.57$. Frogel et al. (1990) also derive 0.57 for an A0 star. Terndrup et al. (1990), from M giants, derive a $E(B - V) = 0.54$. The estimate is, essentially, based on the similarities between NGC6522 and the SGR-I field. No HST observations in the relevant passbands are available for NGC6522. We adopt $E(B - V) = 0.58$.

4.2.2. Baade's window at R.A.=18 03 11.7 δ =-29 51 40.7

This field is situated in the low extinction area called Baade's Window. Stanek (1996) produced a detailed extinction map of this area from OGLE data. The uncertainty, which is systematic, in this determination mainly arises from the zero point. This grid has 30arcsec spacing, and we are cautioned that there may exist further structure in the reddening below this spatial resolution. For the position of the PC1 his map gives $E(V - I) = 0.566$ and $A_V = 1.452$. Using Cardelli et al. (1989) this corresponds to $E(B - V) = 0.49$. Using Holtzman et al. (1995b) this translates to $E(V_{F555W} - I_{F814W}) = 0.59$.

4.2.3. Fields at (l,b)=(3°6,-7°0) and (2°9,-7°95)

These fields are part of two parallel programs and we do not have further information from observations of the extinction. Figure 7 however suggests that they suffer from similar extinctions. Since V_{606} is roughly 0.6 magnitudes brighter than V_{555} the turn-offs for these two fields appear very similar in colour to those of SGR-I and Baade's window. We primarily use these observations for number counts in I_{814} .

4.3. The globular clusters

Two of the clusters, NGC6528 and NGC6553, are situated between us and the Galactic Bulge. The third, NGC5927, is also in the disk but well away from the Bulge line of sight, hence we will only have contamination from disk

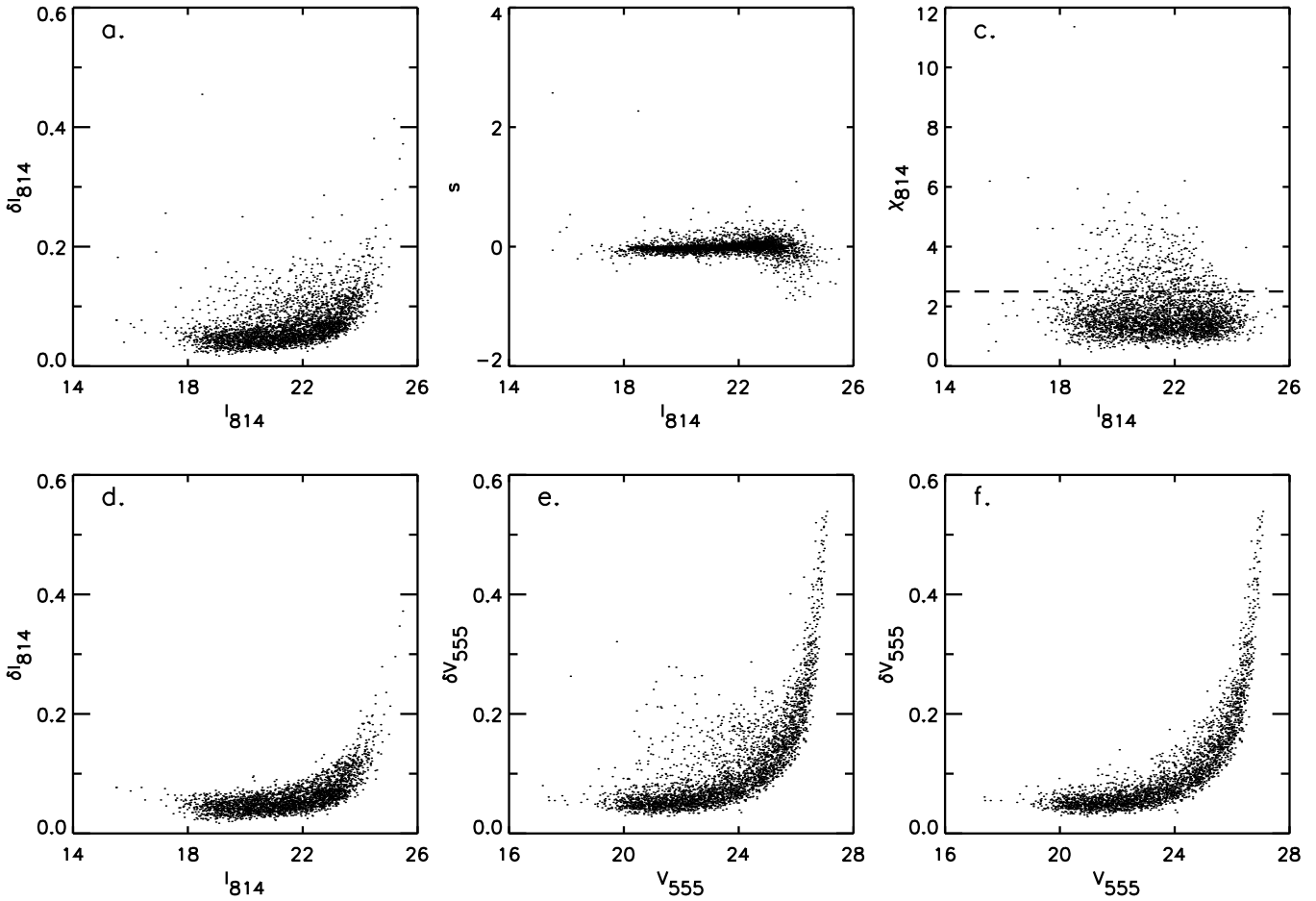


Fig. 4. Diagnostics for the SGR-I field. Figures a., b., and c. show the error, δI_{814} , the sharpness and the χ_{814} as a function of the I_{814} magnitude. In d. we show the same as in a. but when the cut in χ_{814} is imposed (as indicated in c.). Finally in Figures e. and f. δV_{555} are shown as functions of V_{555} magnitudes. In e. without any cuts imposed and in f. when χ_{555} cut at 2.5. Figure d. and f. thus show the distribution of the errors in the final sample of stars in SGR-I colour-magnitude diagram as displayed in Fig. 6.

Table 4. Data for NGC5927 compiled from the literature.

	Value	Ref.	Comment
Core radius	0'.42	Harris (1996)	
$\Delta(m - M)$	16.10	Zinn (1980)	16.6 kpc
	14.52	Djorgovski (1993)	8.0 kpc
[Fe/H]	-0.16	Zinn (1980)	
	-0.30	Zinn & West (1984)	
	-0.32/ -0.64	Rutledge et al. (1997)	Zinn & West (1984) scale/Caretta& Gratton (1997) scale
[Fe/H] _{47Tuc}	+0.57	Cohen (1983)	relative to 47 Tuc at -0.7 dex
Age	10.9 ± 2.2 Gyr	Fullton et al. (1996)	
	15 Gyr	Samus et al. (1996)	
E(B-V)	0.48	Zinn (1980)	
	0.46	Peterson (1993)	
	(0.44) - 0.46	Sarajedini & Norris (1994)	For several solutions for reddening and metallicity

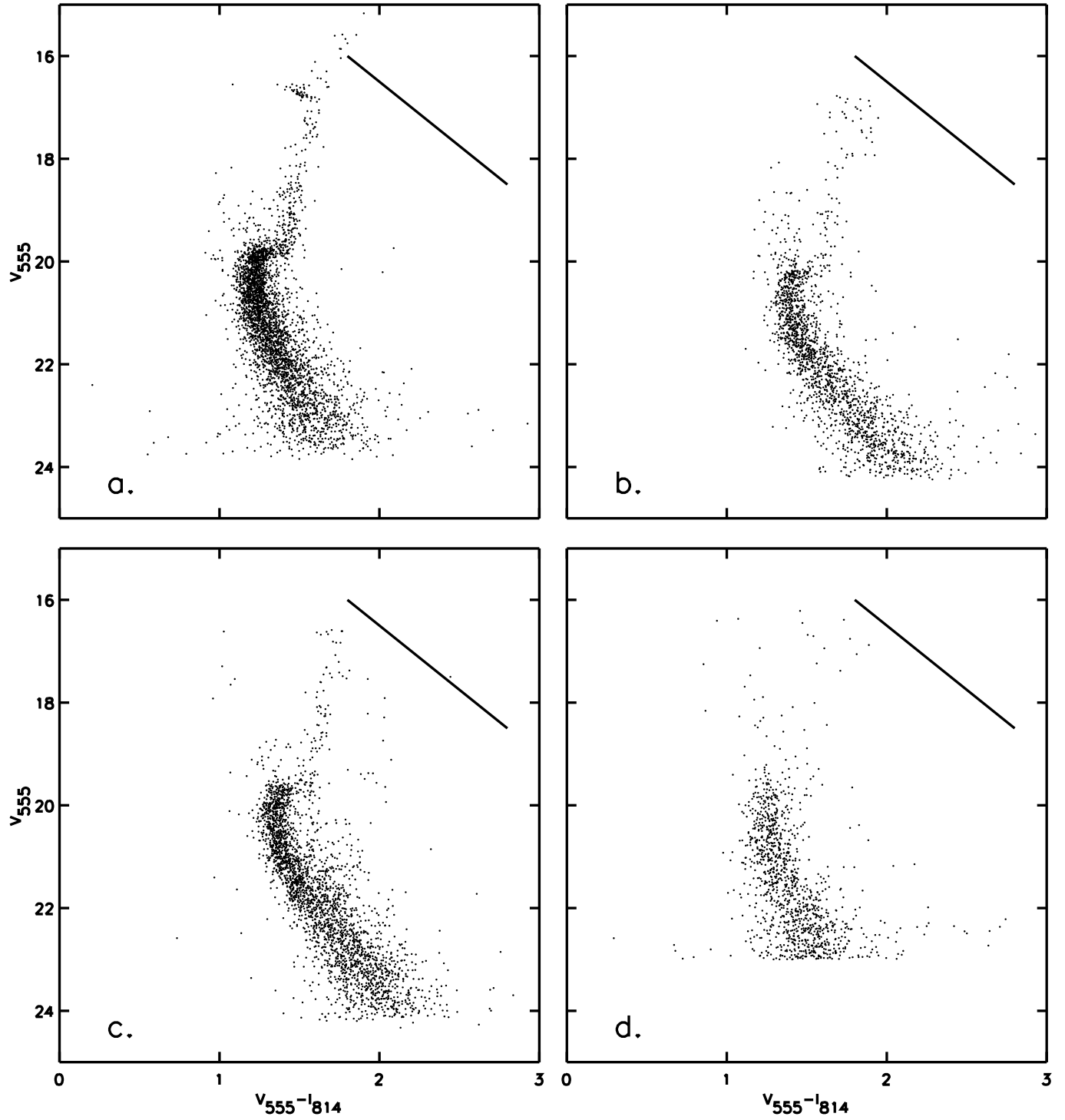


Fig. 5. Colour magnitude diagrams for the cluster fields and the short exposure of Baade’s window. a. NGC5927 short exposure, b. NGC6528 c. NGC6553, and d. BW short exposure. The direction of the reddening vector, as given in Holtzman et al. (1995b), is indicated by a solid line in each diagram. The colour-magnitude diagram for Baade’s window was truncated at $V_{555} = 23$.

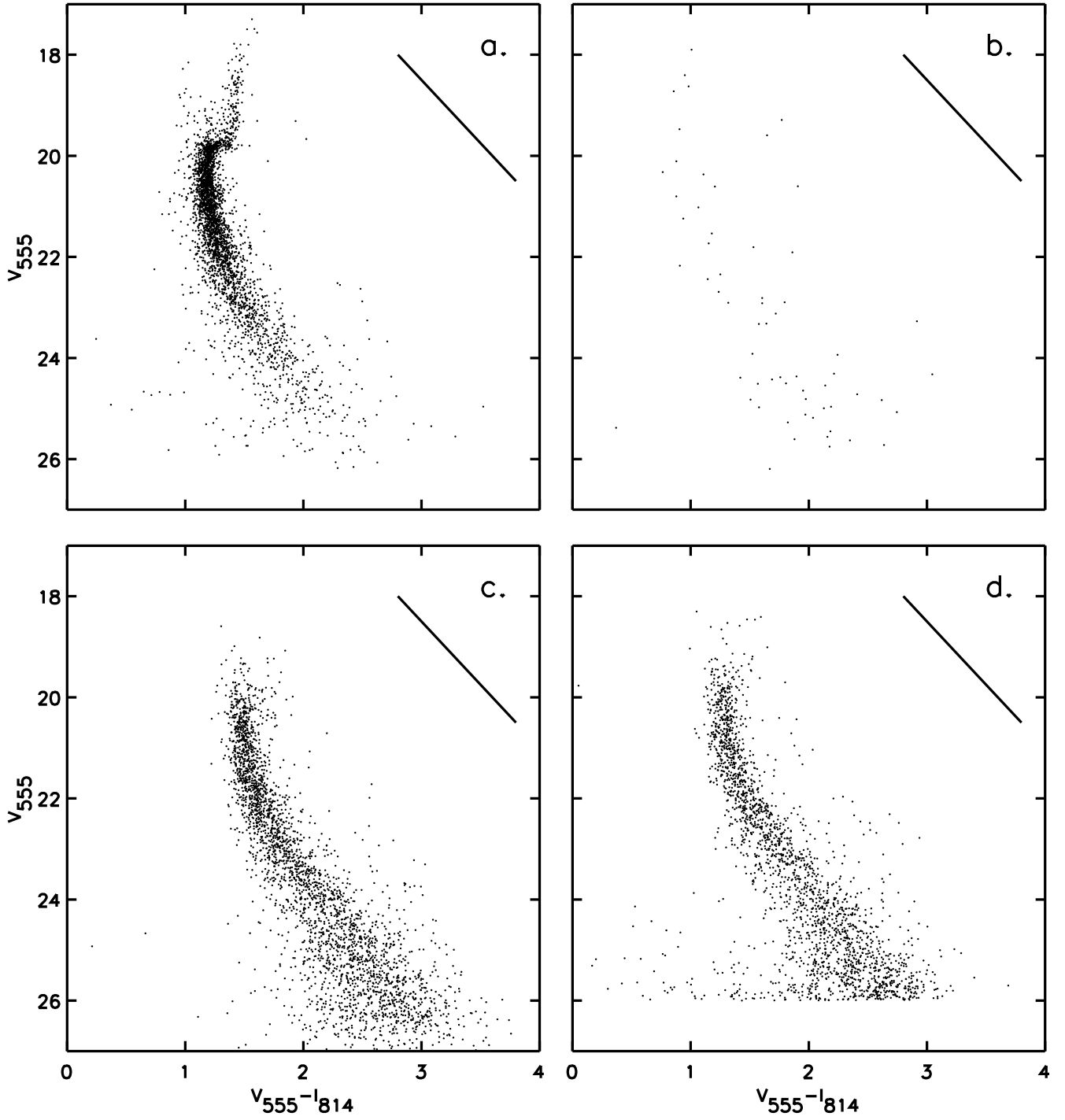


Fig. 6. Colour magnitude diagrams for the two fields and NGC5927. a. NGC5927 long exposure, b. MW-12, c. SGR-I, and d. BW long exposure. The direction of the reddening vector, as given in Holtzman et al. (1995b), is indicated by a solid line in each diagram.

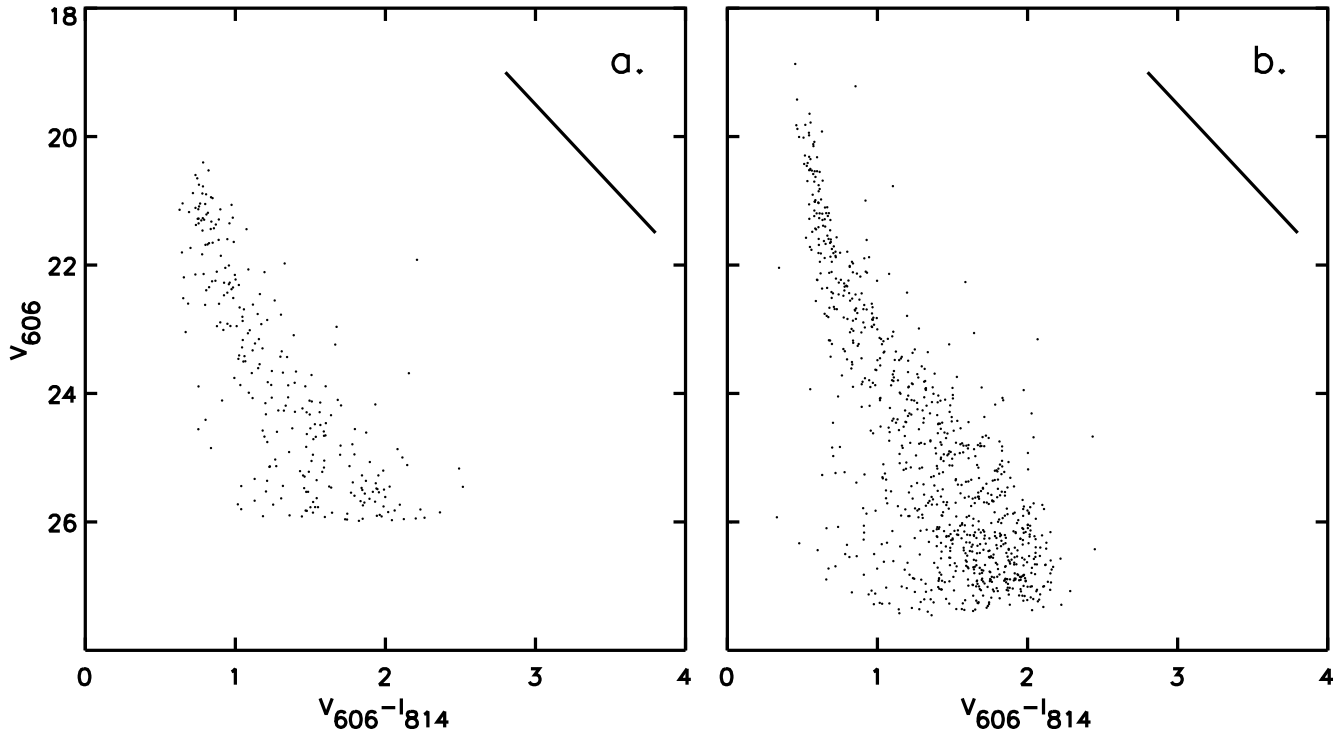


Fig. 7. Colour magnitude diagrams for the two fields observed in F606W and F814W. a. is the field at (l,b)=(2.9,-7.95) and b. at (3.6,-7.2). The colour-magnitude diagram for the field at (2.9,-7.95) has been truncated at $V_{606} = 26$. The direction of the reddening vector, as given in Holtzman et al. (1995b), is indicated by a solid line in each diagram.

Table 5. Data for NGC6528 compiled from the literature.

	Value	Ref.	Comment
Core radius	0'09	Harris (1996)	
Distance	7.5 kpc	Ortolani et al. (1992)	
$\Delta(m - M)$	16.4	Zinn (1980)	19.1 kpc
[Fe/H]	+0.01	Zinn (1980)	
	+0.29	Bica & Patoriza (1983)	
	+0.12	Zinn & West (1984)	
	-0.23	Armandroff & Zinn (1988)	Integrated spectra IR Ca II
	high, sim to NGC6553	Ortolani et al. (1992)	
	-0.23	Origlia et al. (1997)	IR abs. at 1.6 μm
[M/H]	+0.1/ - 0.4	Richtler et al. (1998)	Trippico isochrone/Bertelli isochrone
Z	Z_{\odot}	Bruzual et al. (1997)	
Age	14 Gyr	Ortolani et al. (1992)	metallicity comparable to solar
	12 ± 2 Gyr	Bruzual et al. (1997)	
E(B-V)	0.55	Ortolani et al. (1992)	NGC6553 as reference and $\Delta(m - M)_V = 14.39$
	0.62	Bruzual et al. (1997)	
	0.56	Zinn (1980)	
E(V-I)	0.8/0.6	Richtler et al. (1998)	Trippico isochrone/Bertelli isochrone

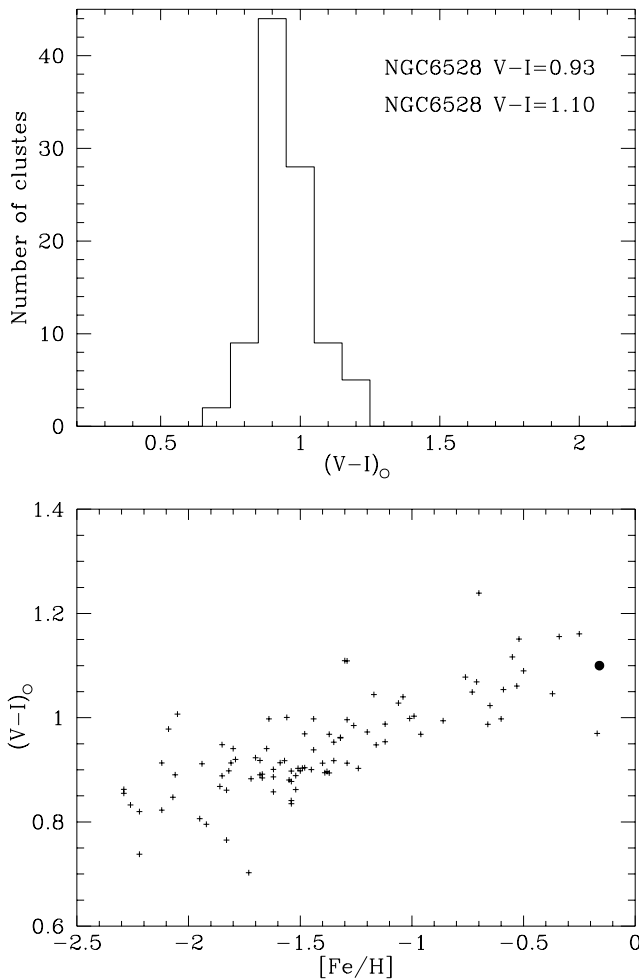


Fig. 8. Histogram showing the distribution of integrated $(V-I)_o$ for all the clusters in Harris (1996) catalogue for which photometry in all passbands are available. We have used the reddening quoted in Harris to calculate the intrinsic colours. The catalogue values of $V-I$ for NGC6528 and NGC6553 are given. Harris give $E(B-V)_{6528} = 0.62$ and $E(B-V)_{6553} = 0.84$. Note that if we used the reddenings quoted in this paper the clusters would in fact become intrinsically even less red. The second panel shows the $V-I$ colours as a function of the $[Fe/H]$ values quoted in Harris. The \bullet in the lower panel indicates the position of NGC6553 with the new iron abundance from Cohen et al. (1999).

stars in this field. All three are thought to be among the more metal-rich globular clusters in the Galaxy (e.g. Rutledge et al. 1997). The cluster kinematics have been interpreted as evidence that the clusters are members of what is called the bulge population of globular clusters (see Minniti 1996 and references therein). We noted above that such assignments do not allow any deduction on the relative properties (ages, etc) of field and cluster stars, given the lack of understanding of the formation of either population.

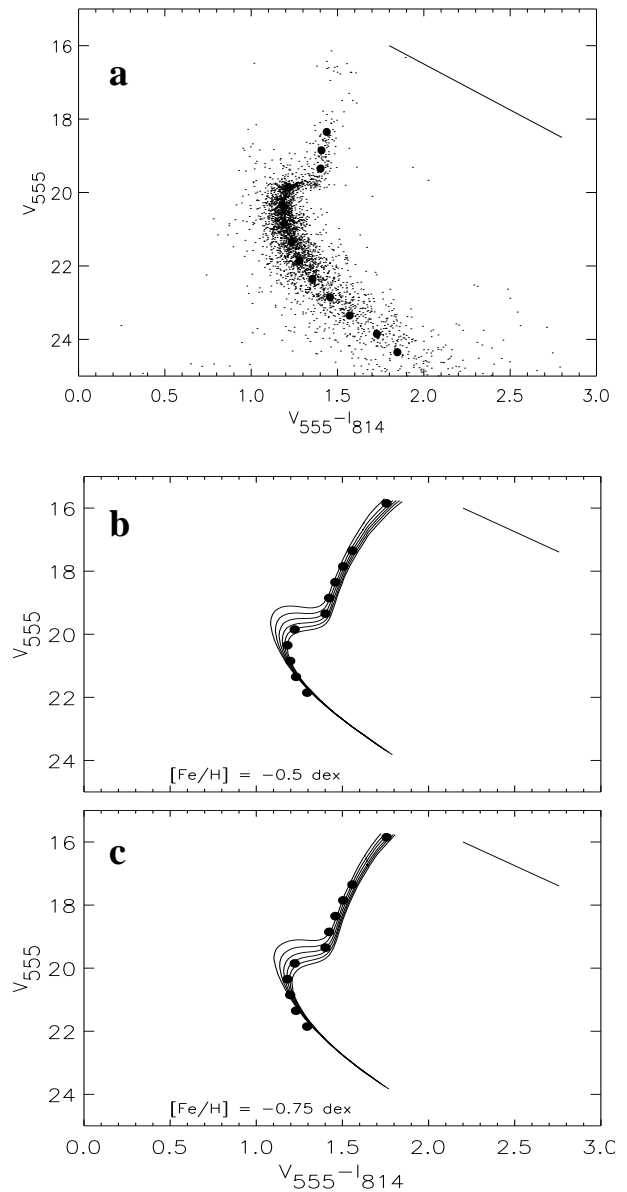


Fig. 9. Colour-magnitude diagrams for NGC5927. In panel a the long exposure. The ridge line used in Sect. 6.1 is over-plotted as heavy dots. In panel b and c are the ridge line shown for the short exposure with isochrones superimposed. Isochrones are for 8, 10, 12, 14, 16, 18 Gyr, Bertelli et al. (1994) and Guy Worthey (private communication). The isochrones have been moved to a distance of 8 kpc and an extinction of $E(B-V) = 0.46$. Reddening vectors are plotted in upper right hand corner. Metallicities as indicated

We have searched the literature for data on the clusters. Several studies are available, both in the visual and the IR as well as spectroscopic studies of individual stars and of the integrated light from the cluster, and are summarized in Tables 4, 5 and 6. References reporting a result are given in preference to later reviews. It is important for our study to understand the metallicities of the clusters and the fields, at least on a relative scale. Large metallicity differences would influence the conclusions from the number counts in Sect. 5.

We note, using the catalogue data by Harris (1996), that the integrated colours for NGC6528 and NGC6553 show them to be “normal” clusters. This is illustrated in Fig. 8, where it is seen that extreme high metal abundances are unlikely, given their integrated colours.

4.3.1. NGC5927

This cluster is situated in the disk well away from the Bulge, and is one of the most metal-rich disk globular clusters known. Fullton et al. (1996) present colour-magnitude diagrams from the same HST/WFPC2 observations as we use. They derive a cluster age of 10.9 ± 2.2 Gyr, using $[\text{Fe}/\text{H}] = -0.24 \pm 0.06$ dex. This makes the cluster 3-5 Gyr younger than many other disk clusters. The lower metallicity found from CaII infrared triplet lines by Rutledge et al. (1997) would imply a higher age. Samus et al. (1996) presented the first deep ground-based *BVI* photometry for the cluster from which they derived an age of 15 Gyr assuming $[\text{Fe}/\text{H}] = -0.49$ dex.

In Fig. 9 we show the ridge-line of NGC5927 with theoretical isochrones for 8-18 Gyr over-plotted. The isochrones have been moved to a distance of 8 kpc and an extinction of $E(B - V) = 0.46$ (see Table 4). From this we infer that $[\text{Fe}/\text{H}] = -0.64$ dex, as derived by Rutledge et al. (1997), is a good fit to the data. Also that a very young age is not likely, but rather 12 – 14 Gyr.

4.3.2. NGC6528

NGC6528 is situated in the line of sight towards Baade’s Window. It has been the subject of two separate studies (Ortolani et al. 1992 and Richtler et al. 1998), as well as figuring in a number of studies of other metal-rich globular clusters (Cohen & Sleeper 1995, Ortolani et al. 1995, Kuchinski et al. 1995, Bruzual et al. 1997). To our knowledge no spectroscopic abundances have been reported.

From the similarities in field and cluster colour-magnitude diagrams, Ortolani et al. (1992) concluded that not only is NGC6528 projected onto the Galactic Bulge but the stellar population is indistinguishable from that of the bulge population. They noted a strongly curved red giant branch, interpreted as evidence for high metallicity, and a tilted horizontal branch. Richtler et al. (1998) could not identify the cluster red giant branch directly in their colour-magnitude diagram due to the combination of the

Bulge population in the observed area and cluster AGB stars. The initial tilt of the horizontal branch was significantly reduced by carefully selecting bulge stars and discarding the field stars. By investigating the membership of the very red giants, $V - I > 3.5$, they conclude that the cluster is indeed situated in front of the general bulge field population and not embedded in it.

Our data do not reach bright enough magnitudes to study the horizontal branch in detail, however, from number counts in Sect. 5 we conclude that our colour-magnitude diagram is significantly contaminated by Bulge stars. Thus, while NGC6528 is possibly not a clean fiducial cluster, it is ideal for our present age-test experiment (see also Sect. 7).

4.3.3. NGC6553

NGC6553 is perhaps the best studied cluster of the three. Ortolani et al. (1990) published the first detailed study of this cluster, which is situated at a projected distance of $\sim 6^\circ$ from the galactic centre and roughly at a distance of 5 kpc from us. Being some 10-20 scale lengths from the Galactic centre, this makes it a marginal ‘bulge’ cluster. However it is often included in such studies (eg Barbuy et al. 1998). Here we will use its colour-magnitude diagram to constrain the number of young stars in the Galactic Bulge, Sect. 5. However, the colour-magnitude itself merits a further discussion here. The work of Ortolani et al has been followed up in the infra red by Davidge & Simons (1994), and by Guarnieri et al. (1997) who present a study based on both optical and infrared observations. The aim with this study is to provide a template for infra red studies of the galactic bulge population.

4.3.4. Differential reddening towards NGC6553?

Our colour-magnitude diagram, in Fig. 5, shows some intriguing and previously not discussed patterns. At $V \sim 21.5$ an apparent second turn-off is seen and more or less parallel to the red of the red giant branch is a second sequence of stars. This sequence is actually visible also in the colour-magnitude diagram in Ortolani et al. (1995), however the apparent turn-off is not. Additionally, this cluster has a well-known ‘tilted’ horizontal branch, with the HB slope lying close to that of the reddening vector, and has a broad main-sequence turn-off.

Can the “extra” giant branch, and the various other anomalies be due to differential reddening of cluster stars? Ortolani et al. (1995) found the reddening to be variable over the PC1, ~ 0.2 magnitudes across the field. The simplest possible test is to see if the CMD anomalies are restricted to one patch of the field that has higher reddening. In Fig. 10 we show the positions of the stars in the “extra” giant branch. It is clear that the stars are evenly distributed over the image and that their positions in the colour-magnitude diagram cannot therefore be due to a

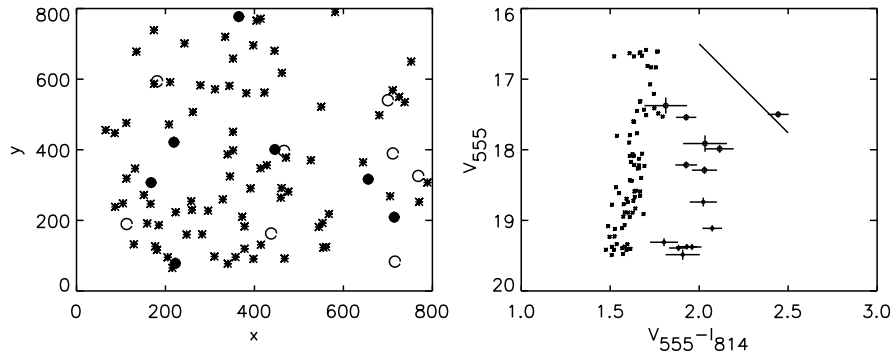


Fig. 10. NGC6553. a. The position on the PCI chip for the stars on the two giant branches. b. Colour-magnitude diagram for the same stars. The direction of the reddening is indicated by a solid line. Open circles denote stars with $V_{555} < 18.5$ and filled circles stars with $V_{555} > 18.5$. Error bars, as given by ALLSTAR, are over plotted for these stars.

simple selective extinction effect. Plausible astrophysical explanations all have difficulties: the obvious explanation, that this is the background Galactic bulge, with some additional reddening, is very difficult to make consistent with the data. An alternative, though also speculative, explanation is that the second giant branch is part of the Sgr dSph galaxy (Ibata et al. 1995). The absence of any such features in Fig.7 for fields closer to the centre of Sgr requires a very non-uniform surface density in the dwarf galaxy. However, even with this explanation, further reddening beyond NGC6553 is required to move it to such red colours.

An explanation of the colour-magnitude data for NGC6553 remains difficult. Reddening which is both patchy and mixed through the cluster remains feasible. A detailed HST (WFPC plus NICMOS) study is required, and is underway. It will be reported elsewhere (Beaulieu et al. 1999, in prep.). In the interim, some reserve in deductions from this cluster is advised.

4.3.5. Spectroscopic abundances

In addition to the metallicities based on photometry and spectroscopy of the Ca II infra red triplet, summarized in Table 6, two studies have obtained high-resolution abundance data for a handful of stars in the cluster. Barbuy et al. (1997) completed the first detailed abundance study and derive Mg, Ti, Si, Ca and Eu abundances as well as Fe abundances for 3 very cool stars. Preliminary results are $[Mg/Fe] \simeq +0.15$, $[Ti/Fe] \simeq +0.3$, $[Si/Fe] \simeq +0.6$, $[Ca/Fe] \simeq 0.0$ and $[Eu/Fe] \simeq +0.3$. The abundance ratios for Mg, Ti, Ca and Eu are similar for those found in metal-rich dwarf stars in the solar neighbourhood (Feltzing & Gustafsson 1998 and Feltzing 1999) while the cluster appears overabundant in Si. This could point to a rapid star formation history, but any interpretation is contradicted by the low Ca abundance, which is not consistent with the other alpha-elements.

Cohen et al. (1999) find that five horizontal branch stars have a mean $[Fe/H]$ of -0.16 dex, which is comparable to the mean abundance in the Galactic Bulge as found by McWilliam and Rich (1994). The horizontal branch stars are preferable to use because their spectra are less

crowded and abundances are therefore more readily extractable than in the very crowded spectra used by Barbuy et al. We will therefore adopt this new high $[Fe/H]$. This is also consistent with the early findings by Cohen (1983) that an underestimate in $E(B - V)$ of as little as $0.^m05$ corresponds to an underestimate in $[M/H]$ of 0.2 dex.

5. The age of the Galactic Bulge

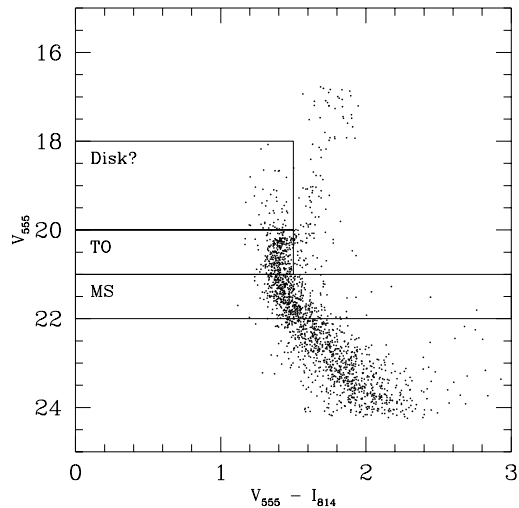


Fig. 11. Definition of windows for NGC6528, Table 7.

In our colour-magnitude diagrams in Fig 5 and 6 there appear to be many stars in the “young stars” and “blue straggler” region, brighter and bluer than the main-sequence turn-off. Because the turn-off region is sensitive to age (Fig. 12) is this evidence for a young stellar population? The turn-off region in these diagrams is also sensitive to foreground contamination, and to bulge blue stragglers. Rather than simply assuming the nature of the stars around the turn-off in the colour-magnitude diagrams of Bulge fields, foreground or a substantial young Bulge population, we test the possibility that they are foreground

Table 6. Data for NGC6553 from the literature.

	Value	Ref.	Comment
Core radius	0'.55	Harris (1996)	
Distance	4.9 kpc	Ortolani et al. (1990)	
$\Delta(m - M)$	16.4	Zinn (1980)	19.1 kpc
	13.6 \pm 0.25	Guarnieri et al. (1992)	5.25 kpc
[Fe/H]	+0.26	Zinn (1980)	
	+0.47	Bica & Pastoriza (1983)	For a discussion of probable error sources see Barbuy et al. (1992) (CNO excess)
	-0.7	Pilachowski (1984)	Spectroscopy of 1 star
	-0.41	Webbink (1985)	
	-0.2 ^{+0.2} _{-0.4}	Barbuy et al. (1992)	Spectroscopy of star III-17
	\geq -0.4	Davidge & Simons (1994)	IR photometry
	-0.29	Zinn & West (1994)	
	-0.55	Barbuy et al. (1997), Barbuy et al. (1999)	Spectroscopy of 3 giant stars
	-0.33	Origlia et al. (1997)	IR abs. at 1.6 μ m
	-0.60	Rutledge et al. (1997)	IR Ca II triplet
	-0.16	Cohen et al. (1999)	from 5 horizontal branch stars
[Fe/H] _{47Tuc}	+0.24/ +0.37	Cohen (1983)	Spectroscopy 5 stars/2 most metal-rich stars, relative to 47 Tuc at -0.7 dex
	+0.10	Cohen & Sleeper (1995)	relative to 47 Tuc at -0.71 dex
Z	Z $_{\odot}$	Bruzual et al. (1997)	
Age		Ortolani et al. (1990)	between 47Tuc and Pal 12
	12 \pm 2 Gyr	Bruzual et al. (1997)	
E(B-V)	0.78	Zinn (1980)	
	\leq 1.0	Ortolani et al. (1990)	
	0.7	Guarnieri et al. (1997)	

Table 7. Number of stars in “boxes”. The first column identifies the fields and clusters, the second the designation, i.e. MS (main sequence), TO (turn off), and Disk, for the box, the third gives the range in V_{555} and the fourth gives the range in $V_{555} - I_{814}$ used for defining the box, then follows the number of stars counted in each box. The last three columns give the relative numbers in the different boxes.

Field		V	V-I	#	Disk/MS	Disk/TO	TO/MS
SGR-I	Disk	18-20	0-1.6	54	0.13	0.20	
(d=3deg)	TO	20-21	0-1.6	268			0.07
	MS	21-22	all	404			
BW	Disk	18-19.7	0-1.35	34	0.12	0.18	
(d=4deg)	TO	19.7-20.7	0-1.4	188			0.07
1000s	MS	20.7-21.7	all	276			
BW	Disk	16(18)-19.7	0-1.35	47(39)	0.15(0.13)	0.24(0.20)	
40s	TO	19.7-20.7	0-1.4	193			0.06
	MS	20.7-21.7	all	307			
NGC6528	Disk	18-20	0-1.5	50	0.11	0.18	
(d=5deg)	TO	20-21	0-1.5	278			0.06
	MS	21-22	all	473			
NGC6553	Disk	-19.5	0-1.44	26(31)	0.04(0.05)	0.07(0.08)	
(d=6deg)	TO	19.5-20.5	0-1.44	397			0.06
	MS	20.5-21.5	all	667			
NGC5927	Disk	18-19.6	0-1.3	52	0.06	0.06	
(d=35deg)	TO	19.6-20.6	0-1.3	809			0.09
	MS	20.6-21.6	all	889			

disk contamination. This is done by quantifying their spatial distribution, since foreground disk stars will be distributed on the sky differently than are bulge stars, of whatever age. The key to this experiment is our consideration of fields in a variety of directions, and in particular use of the cluster NGC5927, which is at longitude 34° , far from the bulge.

We defined three “windows” in our colour-magnitude diagrams in which we performed number counts. The location of the windows was decided upon by inspecting the colour-magnitude diagrams of SGR-I and NGC6528. We defined three windows; one corresponding to stars above the turn-off (young bulge and/or foreground disk and/or blue stragglers), one at the turnoff of an old population and one on the bulge main sequence, as illustrated in Fig. 11. The colour and magnitude limits were then adjusted for each field and cluster to take distance and reddening differences into account, following Table 7.

We first compare the counts for the two clusters, NGC6553 and NGC5927, one near the bulge, one far out in the disk. For these two clusters, The relative number of stars that are either young or are foreground disk stars and stars that are thought to belong to the Bulge, called “Disk/MS” in the table, is constant between the fields, while the absolute number is roughly constant. This is direct evidence that the counts in the disk box are dominated by true disk stars and not true bulge stars. Further direct evidence that the “disk” stars are disk, is the near constancy of their surface density in the inner bulge fields.

In this part of the diagram the star numbers do not change with l, b as they would if we were seeing a young Bulge population. The COBE Bulge has a scale length of $\sim 1^\circ$ (Binney, et al. 1997) and hence the number counts would change significantly over the area studied.

The ratio of disk to main sequence and turn-off stars for NGC6528 is different to that for the other two clusters, suggesting that for this cluster the colour-magnitude diagram is significantly affected by field contamination, perhaps explaining some of the apparent anomalies noted in earlier analyses of these HST images (Ortolani et al. 1995).

Table 8. Number counts in I_{814} for the four fields. Their relative numbers are compared with simple predictions using the E2 model of the Galactic Bulge density distribution from Dwek et al. (1995).

Field	ΔI_{814}	#	rel. SGR-I	Model
SGR-I	20.0-21.0	536	–	–
BW	19.5-20.5	372	0.69	0.62
	20.0-21.0	328	0.61	
u811	20.0-21.0	52	0.10	0.11
Deep	20.0-21.0	44	0.08	0.09

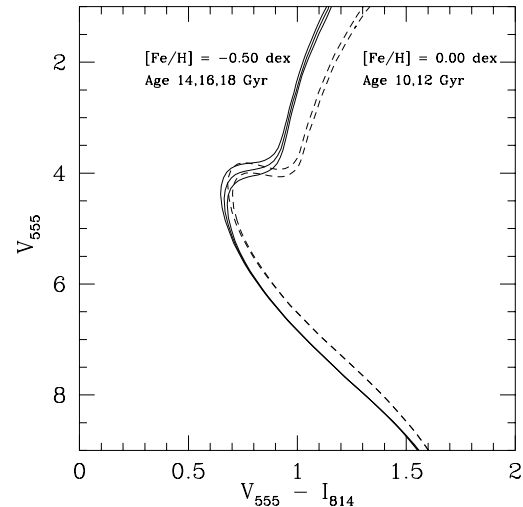


Fig. 12. Illustration of the age-metallicity degeneracy around the turn-off. Isochrones are from Bertelli et al. (1994), in the HST passbands courtesy of G. Worthey.

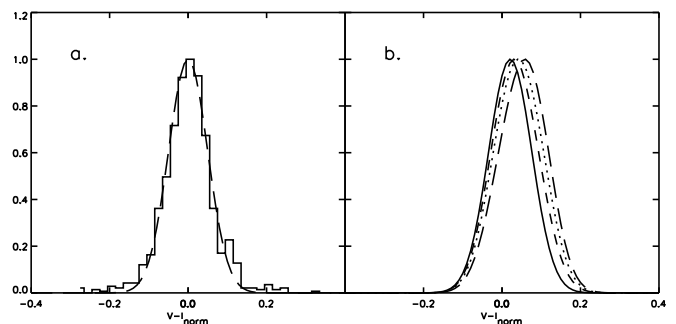


Fig. 13. In panel a. we show the colour distribution for stars in NGC5927 with $20.2 \leq V_{555} \leq 21.2$. The histogram has been moved so that its mean colour ($V - I_{\text{norm}}$) is zero. To this histogram a Gaussian is fitted, shown by the dashed line. This Gaussian defines the colour distribution in a single stellar population, convolved with our photometric errors. A colour difference of 0.07 in magnitude corresponds to a change in $[\text{Fe}/\text{H}]$ of 0.3 dex (at -0.3 dex and 0.0 dex). Two Gaussians separated in colour by the equivalent of a 0.3 dex metallicity difference are added to make up a reasonable representation of the colour distribution in Baade’s window (see text). This is plotted in b. To the Gaussian representing Baade’s window a third population at +0.3 dex is added in different proportions, to illustrate the effect on the observed colour distribution of a very metal-rich population. The three curves are: short dashed line 50% stars added, dotted line 100% stars added and long dashed line 200%.

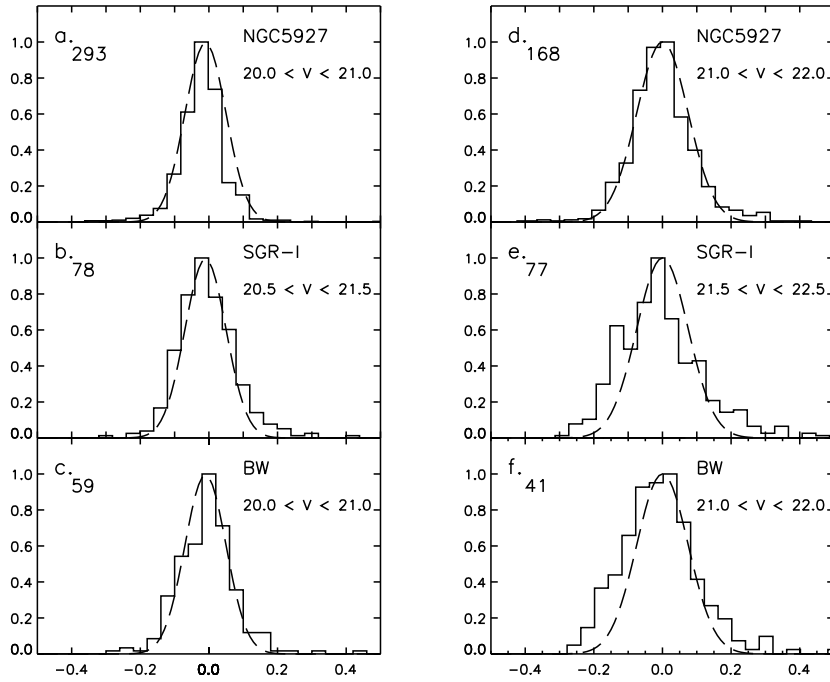


Fig. 14. Normalized histogram of the colour distribution of stars in magnitude slices for NGC5927, SGR-I and the deep exposure of Baade’s window. The slices are made in V_{555} , with magnitude ranges appropriate for reddening and distance in each line of sight. The magnitude ranges are: panels a and c are for 20-21, b for 20.5-21.5, d and f for 21-22, and e for 21.5 -22.5.

The spatial distribution of the number counts in I_{814} in the four deep fields are consistent with results from simple simulations using the E2 model of the Galactic Bulge in Dwek et al. (1995) (Table 8). We present two counts for Baade’s window. This field has the lowest extinction and we would expect the counts between $19.5 \lesssim I_{814} \lesssim 20.5$ to be comparable with the counts in SGR-I between 20.0 and 21.0. However, for comparison we also give the counts in the same apparent magnitude bin for Baade’s window. As can be seen the difference is small, but consistent with Baade’s window having an extinction ~ 0.3 magnitudes less than that towards SGR-I.

We conclude that the apparent evidence for a significant young Bulge population in our colour-magnitude diagrams is an artifact of disk contamination. Correcting the observed colour-magnitude diagrams, using the results for NGC5927, removes all the stars above and to the blue of the turnoff. That is, there is no evidence in these HST/WFPC2 data for a significant age range in the bulge population.

This tight limit, extending the previous results of Ortolani et al. that the bulk of the bulge is old, is somewhat surprising. What happens to all the young stars forming in the inner disk? We emphasize however, that available limits still allow an age range of several Gyr, especially so, as discussed below, if there is an age-metallicity relation in the bulge stars.

5.1. Can we resolve the metallicity distribution function?

We now consider if we are able to use the apparent width of the main-sequences in the colour-magnitude diagrams to constrain the width of the stellar metallicity distribution function. Recall, from Fig. 12 that a younger metal-

richer population can hide in the turn-off region. It should, however, show up on the main sequence, if the statistics are good enough.

In Fig. 13 we show a slice histogram for NGC5927 for all stars between V_{555} 20.2 and 21.2 and a Gaussian fitted to it. We use this Gaussian as a representation of the apparent colour distribution including measurement errors of a single stellar population in our data. A difference of 0.07 in colour corresponds to a change in $[\text{Fe}/\text{H}]$ of 0.3 dex. Two Gaussians separated by 0.3 dex are added to make up the Gaussian drawn with a full line. This should be a reasonable representation of the colour distribution in Baade’s window (see text). To the Gaussian representing Baade’s window we add a third population at +0.3 dex. As is clear from the figure, to be able to resolve a metal-rich extra population, that population has to be large in numbers relative to the metal-poor one, and enough stars have to be observed so that the histograms can be constructed with small enough bins (~ 0.02). This is not the case here.

In Fig. 14 the histograms have been moved so that the mean colour for each slice is centred at 0. We have fitted a Gaussian to the two histograms for NGC5927. This Gaussian is reproduced in the panels showing the histograms for SGR-I and Baade’s window. From this we conclude that there is some evidence for a larger spread in $V - I$ in the fields than in the cluster. In particular, the slice at a fainter V_{555} show a larger spread towards the blue, for the two field populations than for the cluster, consistent with a broad metallicity distribution function with a tail to metal-poor stars. The metal-rich (red) sides of the histograms are however too poorly determined for useful conclusions.

6. Is there a detectable metallicity gradient?

In order to check a possible metallicity gradient, we compare the colour-magnitude diagrams of the Baade’s window and SGR-I field. This is a particularly robust method, since we are not sensitive to incompleteness at the faint end of the ridge lines, the colour-magnitude diagrams being comparably complete.

6.1. The metallicity in Baade’s window

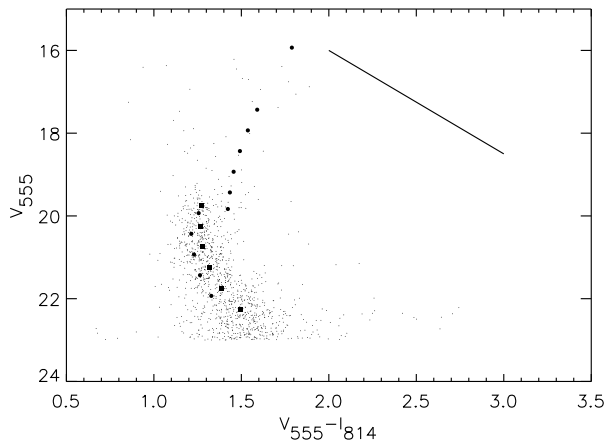


Fig. 15. The CMD for Baade’s Window is shown, together with its own ridge line (fainter than $V_{555} \sim 20$, open squares). The solid points (\bullet) are the ridge line constructed from the colour-magnitude diagram of NGC5927, shifted along the reddening line appropriately.

Figure 15 shows the colour-magnitude diagram from the short exposure of Baade’s window with its own ridge line, and also the ridge line derived from the NGC5927 short exposure data. The ridge line of the cluster has been moved along the reddening line to account for the differences in reddening for the two fields. We observe that the both the main sequence and the giant branch of the field population(s) are redder than those of the cluster. From this we conclude that the mean metallicity of Baade’s window is ~ 0.3 dex higher than that of the cluster. This is in good agreement with results from spectroscopic studies.

6.2. The Bulge metallicity gradient

The most robust way to compare colour-magnitude diagrams is to construct a ridge line for each field. The ridge lines can then be moved to compensate for differential reddening effects, and compared to appropriate isochrones. This is illustrated in Fig. 16. We see, in panels (a) and (b), that adopting literature values for the reddening, and attributing all the resulting difference between the ridge lines to metallicity, implies a difference of 0.5 dex in metal

abundance, which corresponds to 3.2 dex/kpc, assuming a distance of 8 kpc to the Galactic Bulge.

However, the relative reddening between the fields may well be in error. We thus test two further hypotheses. First, that there is no significant metallicity gradient, but there is an age gradient. This is shown in Fig.16 panel (c), where one sees that an age gradient of ~ 6 Gyr over 0.14 kpc is required, a result we consider implausible.

We therefore try a further experiment, assuming the reddening is unknown, and is a free parameter to be determined. In this case we can derive a lower limit to any real age or abundance gradients, if we conservatively assign as much as is possible of the differences between the colour-magnitude diagrams to reddening, while fitting the two ridge lines using their overall morphology. This is shown in panel (d) of Fig. 16. No significant residual systematic difference between SGR-I and Baade’s window remains.

Using the isochrones by Bertelli et al. (1994) our best estimate of any allowed difference is $\lesssim 0.25$ dex. We conclude that there is no strong evidence for an abundance gradient between Baade’s window, at projected distance from the centre of 550 pc, and SGR-I, at projected distance 412 pc, assuming a distance of 8 kpc for the Bulge. The upper limit on the amplitude of any abundance is $\lesssim 0.2$ dex, corresponding to $\lesssim 1.3$ dex/kpc. This value may be compared with the recent suggested detection, by Frogel et al. (1999), of a gradient of amplitude 0.5dex/kpc.

7. Discussion

Our conclusion that the Galactic Bulge is predominately old is in conflict with those of Vallenari et al. (1996) and Holtzman et al. (1993). Both these studies found evidence for a substantial (up to 30%) young stellar population in Baade’s window. Also Kiraga et al. (1997), from OGLE data, concluded that the disk stellar population in Baade’s window is old, while the true Bulge stars have a bluer turn-off implying a younger age than 47 Tuc. These results are based on Baade’s window only. The strength of our study is that it utilizes five different line of sight. Our use of data for the cluster NGC5927 is of considerable value, since this cluster is situated in the disk well away from the sight line towards the Galactic Bulge. Accordingly the contamination present in this colour-magnitude diagram must arise from foreground disk stars. We show that the relative and absolute number counts in this cluster show the same pattern as those in the Bulge fields, showing that the stars previously identified with a substantial (or exclusively) young stellar population in the Galactic Bulge are in fact foreground disk stars. Holtzman et al. (1993) note that their interpretation of the data would likely change substantially if for example the reddening estimates are in error. Our results are mainly robust against such errors. Our results are also in accordance with ground-based studies, especially in the IR, which have found no evidence for a substantial young stellar population in the Galactic

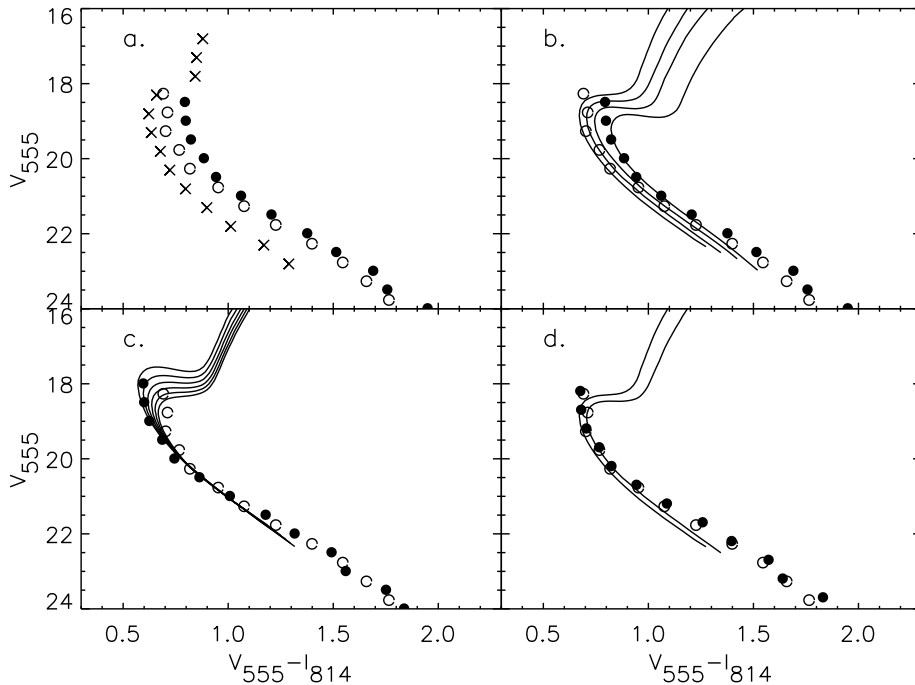


Fig. 16. Each of the 4 panels shows the comparison of the ridge lines for SGR-I (filled circles) and Baade’s window, (open circles). Panel (a) presents the ridge lines as observed, corrected according to the reddenings cited in the literature. This panel also shows the ridge line for NGC5927, (\times). In (b) we also over plot a set of 14 Gyr old isochrones for $[Fe/H] = -0.5, -0.25, 0.0, +0.25$ dex, illustrating the apparent large abundance gradient implied by these adopted reddenings. In panel (c) the ridge lines as observed are moved to optimize agreement between the lower part of the two main sequences. Isochrones for $[Fe/H] = -0.25$ dex and 8, 10, 12, 14, 16, and 18 Gyr (Bertelli et al. 1994 and Worthey private communication) are over-plotted, illustrating the large age gradient implied by this method. In panel (d) the ridge lines are shifted to optimize an overall fit of the morphology. 14 Gyr isochrones for $[Fe/H] = -0.5$ and -0.25 dex are over-plotted to indicate the sensitivity to abundance gradients in this case.

Bulge (e.g. Terndrup 1988, Tiede et al. 1995, Frogel et al. 1990).

The first HST analysis of the stellar populations in Baade’s Window which deduced an old age for the bulk of the bulge stars is that of Ortolani et al. (1995). We use the same HST data, and some other archive data, to provide a direct test of a critical assumption underlying that study, and to extend the analysis to search for gradients in metallicity and/or age. By further removing from the analysis the assumption that the ‘bulge’ globular clusters are a true tracer of the age and metallicity of the field stars, we restrict the analysis to the mean bulge star: the metal rich bulge stars, those above about solar abundance, may be substantially younger than the bulk of the bulge.

Ortolani et al. (1995) observed two ‘bulge’ globular clusters, NGC6553 and NGC6528, with HST/WFPC2. By comparing ridge lines of these globular clusters with that of the metal-rich globular cluster 47 Tuc they concluded that the ‘bulge’ clusters have ages comparable to the halo globular clusters. They then compared the V-band luminosity function of all stars observed in Baade’s Window with the V-band luminosity function observed for NGC6528, concluding that “the main sequence luminosity functions also coincide with extremely high precision in the brighter, age-dependent part that is less affected by incompleteness and field contamination (that is, $19.5 \lesssim V \lesssim 20.5$)”. As is illustrated clearly in our colour-

magnitude data for NGC6528 this part of the apparent magnitude range is indeed heavily contaminated by foreground disk stars, which appear as if they are young bulge stars. Why did these stars not vitiate the Ortolani et al analysis? The explanation is that analyses based only on luminosity functions are valid if and only if the field contamination is exclusively foreground disk, and that there is no significant young bulge population. In that case, the cluster luminosity function is in error in just the same way as is the field data, and so the two errors compensate. In fact, the luminosity function method can be justified only *post hoc*, after an analysis of the type reported here. We confirm that Ortolani et al. (1995) were correct in that assumption.

The observational study of the inner bulge is further confused by the distinct possibility that the very centrally-concentrated “infra-red bulge” seen by IRAS and COBE is not related in a simple way, if at all, to the larger “optical bulge” studied further from the centre (Ibata & Gilmore 1995a, 1995b; Wyse et al. 1997, Unavane & Gilmore 1998, Unavane et al. 1998). Recent studies of external galaxies (Carollo 1999) show that central nuclei are common in bulges, and also that bulges have a diversity of properties. Optical studies in the Milky Way have been restricted to Baade’s window and beyond, ≥ 4 COBE scale lengths from the centre. Here we compare Baade’s window with the low extinction window called SGR-I, roughly at the

limit of optical observations, at $b = 2^\circ 6$, testing to see if the inner and outer Galactic Bulge have the same stellar population(s).

We deduce an upper limit to a metallicity gradient of $\lesssim 1.3$ dex/kpc. Is such an amplitude surprising? Let us consider two distinct possibilities which show that such a result is plausible.

The COBE Bulge has a scale height of ~ 150 pc, and could be interpreted as evidence for a separate component superimposed on top of the optical Bulge. Further evidence that this may indeed be a separate entity (the 'nucleus'?) is provided by the fact that both luminosity and kinematical models (eg Kent 1992) which describe well the outer bulge under-predict the light in the very central part of the Galactic Bulge. At the position of the SGR-I window, at 3 COBE scale lengths from the Galactic Centre we are just beginning to pick up the IR Bulge. It is quite plausible that this centrally condensed structure is considerably more metal-rich than the underlying, larger, optical Bulge which is the main contributor to the stellar population(s) in Baade's window, at $\langle [Fe/H] \rangle = -0.3$ dex.

These results are supported by recent studies of OH/IR stars (Sevenster, et al. 1997). OH/IR stars, which are oxygen-rich, cool giant stars in their final stages of evolution, trace basically all stars with a main-sequence mass of $1 - 6M_\odot$ and can be reliably detected through their OH maser emission at 1612 MHz. This makes them ideal tracers of the underlying stellar population. They are intermediate age or old, and should therefore be dynamically relaxed and trace the global gravitational potential. These stars are distributed in the central Bulge with a scale height $\lesssim 100$ pc (Sevenster et al. 1997).

We also note the fact that star-forming regions such as Sgr B exist shows that star-formation is still going on in the Galactic Bulge on scales of 50-100 pc. This is yet further evidence that we could expect the central parts of the Galactic Bulge to be more metal-rich than the outer edges of the Galactic Bulge. There remains perhaps no more than a semantic distinction between continuing formation of the central Disk and the central Bulge on such small scale lengths and recent times.

In conclusion, both large scale modeling of the dynamics in the Bulge and specific tracers show there to be structure in the stellar populations at scales below those of the optical Bulge. The central parts are a highly dissipated self-enriching part of the Galaxy which is at least partially young.

8. Conclusions

We demonstrate how deep images with high spatial resolutions, only available since the advent of HST, enable us to determine the properties of the Galactic Bulge stellar population(s). In this we have used three measures;

- number counts - to search for a young stellar population
- histograms - to search for a metal-rich population
- comparison of ridge lines - to derive metallicities and look for internal differences, i.e. gradients in age and metallicity

In particular we find that

- our results are consistent with no significant young stellar population in the Bulge, some 500pc, or 2-5 scale lengths, from the centre, contrary to some previous studies;
- the Galactic Bulge has a mean metallicity equal to that of the old disk;
- there is marginal evidence for a central metallicity gradient;
- the colour-magnitude diagram of NGC6553 is complex, requiring care in photometric analyses of this cluster.

Acknowledgements. The UK HST support group in Cambridge, Rachel Johnson and Nial Tanvir, are thanked for numerous discussions on HST/WFPC2 and the best way to extract stellar photometry.

To produce Fig.8 we have use the online version of the Harris (1996) catalogue.

SF acknowledges financial support from the Swedish Natural Research Council under their postdoc program.

References

- Armandroff T.E., Zinn R., 1988, AJ 96, 92
 Barbuy B., Castro S., Ortolani S., Bica E., 1992, A&A 259, 607
 Barbuy B., Ortolani S., Bica E., Renzini A., Guarnieri M.D., 1997, in "Fundamental Stellar Properties: the Interaction between Observation and Theory", Bedding, T.R., Booth, A.J., Davies, J. (eds.), page 203
 Barbuy B., Bica E., Ortolani S., 1998, A.&A 333, 117
 Barbuy, B., Renzini, A., Ortolani, S., Bica, E., Guarnieri, M. D., 1999, A&A 341, 539
 Bertelli G., Bressan A., Chiosi C., Fagotto F., Nasi E. 1994, A&AS 106, 275
 Bica E.L.D., Pastoriza M.G., 1983, Ap&SS 91, 99
 Binney J., Gerhard O., Spergel D., 1997, MNRAS 288, 365
 Bruzual G.A., Babruy B., Ortolani S., Bica E., Cuisinier F., Lejeune T., Schavon R.P., 1997, AJ 114, 1531
 Cardelli J.A., Clayton G.C., Mathis J.S., 1989, ApJ 345, 245
 Carollo, M., 1999 ApJ 523 566
 Cohen J.G., 1983, ApJ 270, 654
 Cohen J.G., Sleeper C., 1995, AJ 109, 242
 Cohen J.G., Gratton R.G., Behr B.B., et al., 1999, astro-ph/9904238
 Davidge T.J., Simons D.A., 1994, AJ 107, 240
 Djorgovski, S., 1993, in Structure and Dynamics of Globular Clusters, ASP Conf. Ser. Vol. 50, Djorgovski. S.G. and Meylan G. (eds.), p. 373
 Dwek R., G.Arendt, R. G., Hauser, M. G., Kelsall, T., Lisse, C. M., et al., 1995, ApJ 445, 716
 Feltzing 1998, in Highlights in astronomy 11, J Anderssen (ed.), Kluwer

- Feltzing S, Gustafsson B, 1998, *A&AS* 129, 237
- Frogel J.A., Terndrup D.M., Blanco V.M., Whitford A.E., 1990, *ApJ* 353, 494
- Frogel, J.A., Tiede, G.P., Kuchinski, L.E., 1999, *AJ* 117, 2296
- Fullton L.K., Carney, B. W., Olszewski, E. W., Zinn, R., Demarque, P., et al., 1996, in *Formation of the galactic halo... Inside and out*, ASP conf Series, vol 92, H Morris & A Sarajedini (eds.), p269
- Glass I.S., Whitlock P.A., Catchpole R.M., Feast M.W., 1995, *MNRAS* 273, 383
- Glass, I., Ganesh, S., Alard, C. et al., 1999 *MNRAS* 308 127
- Gnedin, O. Y., Ostriker, J.P., 1997 *ApJ* 474 223
- Guarnieri M.D., Montegriffo P., Ortolani S., Moneti A., Barbuy B., et al., 1995, *ESO Msngr* 79, 26
- Guarnieri, M. D., Ortolani, S., Montegriffo, P., Renzini, A., Barbuy, B., et al., 1998, *A&A* 331, 70
- Guarnieri M.D., Renzini A., Ortolani S., 1997, *ApJL* 477, 21
- Harris W.E. 1996, *AJ* 112, 1487
- Harris W.E. 1998, in *Galactic Halos: A UC Santa Cruz Workshop*, D. Zaritsky
- Holtzman J.A., Light R.M., Baum W.A., Worthey G., Faber S.M. et al. (eds.), 1993, *AJ* 106, 1826
- Holtzman J., Hester J.J., Casertano S., Trauger J.T., Watson A.M., 1995a *PASP* 107, 156
- Holtzman J.A., Burrows J., Casertano S., Hester J.J., Trauger J.T., 1995b, *PASP* 107, 1065
- Ibata R., Gilmore G., 1995a, *MNRAS* 275, 591
- Ibata R., Gilmore G., 1995b, *MNRAS* 275, 605
- Ibata R., Gilmore G., Irwin M., 1995, *Nature* 370, 194
- Kent S.M., 1992, *ApJ* 387, 181
- Kiraga M, Paczynski B, Stanek K, 1997, *ApJ* 485, 611
- Kuchinski L.E., Frogel J.A., Terndrup D.M., 1995, *AJ* 109,1131
- McWilliam A, Rich R.M., 1994, *ApJS* 91, 749
- Minniti D., Olszewski E.W., Liebert J., White S.D.M., Hill J.M., et al., 1995, *MNRAS* 277, 1293
- Minniti D., 1996, *ApJ* 459, 175
- Ng. Y.K., Bertelli G., Chiosi C., Bressan A., 1996, *A&A* 310, 771
- Omont, A., S. Ganesh, C. Alard, et al., astro-ph/9906489 and *A&A* in press 1999
- Origlia L., Ferraro F.R., Fusi Pecci F., Oliva E., 1997 *A&A* 321, 859
- Ortolani S., Barbuy B., Bica E., 1990, *A&A* 236, 362
- Ortolani S., Bica E., Barbuy B., 1992, *A&AS* 92, 441
- Ortolani S., Renzini A., Gilmozzi R., Marconi G., Barbuy B., et al., 1995, *Nature* 377, 701
- Ortolani S, Gilmozzi R., Marconi G., Barbuy B., Bica E., et al., 1996, in *Formation of the galactic halo... Inside and out*, ASP conf Series, vol 92, H Morris & A Sarajedini (eds.), p96
- Peterson, C.J., 1993, in *Structure and Dynamics of Globular Clusters*, ASP Conf. Ser. Vol. 50, Djorgovski. S.G. and Meylan G. (eds.), p. 337
- Pilachowski C.A., 1984, *ApJ* 281, 614
- Richtler T., Grebel E.K., Subramaniam A., Sagar R., 1998, *A&AS* 127, 169
- Rosenberg, A., saviane, I., Piotto, G., & Aparicio, A., 1999 *AJ* 118 2306
- Rutledge G.A., Hesser J.E., Stetson P.B., 1997, *PASP* 109, 907
- Sadler E.M., Rich R.M., Terndrup D.M. 1996, *AJ* 112, 171
- Samus N., Kravtsov, V., Ipatov, A., Smirnov, O., Alcaïno, G., et al., 1996, *A&AS* 119, 191
- Sarajedini A., Norris J.E., 1994 *ApJS* 93, 161
- Sevenster, M., Dejonghe, H., Habing, H., 1997, *A&A* 299, 689
- Silk J., Wyse R. 1993, *PhR*. 231, 293
- Stanek K.Z., 1996, *ApJ* 460, L37
- Stetson P.B., VandenBerg D.A., Bolte M., 1996, *PASP* 108, 560
- Terndrup D.M. 1988, *AJ* 96, 884
- Terndrup D.M., Frogel, J.A., Whitford, A.E. 1990, *ApJ* 357, 453
- Tiede, Glenn P., Frogel, Jay A., Terndrup, D. M., 1995, *AJ* 110, 2788
- Unavane M., Gilmore G. 1998, *MNRAS* 295, 145
- Unavane M. Gilmore G, Epchtein N., Simon G, Tiphene D., et al. 1998, *MNRAS* 295, 119
- Vallenari, A., Chiosi, C., Bertelli, G., Ng, Y.K, 1996, in "The Galactic Centre" ASP Conf.Ser.102, Gredel, R. (ed.), page 320
- VandenBerg D.A., Bolte M., Stetson P.B., 1990, *AJ* 100, 445
- VandenBerg D.A., Bolte M., Stetson P.B., 1996, *ARA&A* 34, 461
- Walker A.R., Mack P., 1986, *MNRAS* 220, 69
- Webbink R.F., 1985, in *Dynamics of Star Clusters*, IAU Symp. 113, J Goodman, P Huts (eds.), p541
- Wyse R.F G., Gilmore G, 1995, *AJ* 110, 2771
- Wyse R., Gilmore G., Franx M., 1997 *ARA&A* 35, 637
- Zinn R., 1980, *ApJS* 42, 19
- Zinn R., 1996 in *Formation of Galactic Halo ... Inside and Out*, ASP Conf. Series, vol. 92, H. Morrison, A. Sarajedini (eds.), p211
- Zinn R., West M., 1984, *ApJS* 55, 45